JACS
JOURNAL OF THE AMERICAN CHEMICAL SOCIETY

Perspective

pubs.acs.org/JACS

# Chemistry Makes Graphene beyond Graphene

Lei Liao, Hailin Peng,* and Zhongfan Liu*

Center for Nanochemistry, Beijing Science and Engineering Center for Low Dimensional Carbon Materials, Beijing National Laboratory for Molecular Sciences, College of Chemistry and Molecular Engineering, Peking University, Beijing 100871, P. R. China

**ABSTRACT:** Although graphene is extremely inert in chemistry because of the giant delocalized $\pi$ electron system, various methods have been developed to achieve its efficient chemical modification. Covalent chemistry is effective to modulate the physical properties of graphene. By converting the $sp^2$ hybridized carbon atoms to $sp^3$ ones, new two-dimensional (2D) materials and 2D superlattices with fascinating features beyond mother graphene could be built from the graphene scaffold, greatly expanding the graphene family and its attraction. In this Perspective, the power of covalent chemistry is demonstrated from the viewpoint of tailoring graphene's energy band structure as well as creating new 2D materials and 2D superlattices. A specific focus is laid on the general consideration and understanding of covalent graphene chemistry toward electronic devices and material science.

Graphene, a typical two-dimensional (2D) atomic crystal, has attracted great attention because of its various fascinating properties with ultrathin structural feature. The ultrahigh carrier mobility (~200,000 $cm^2/V{\cdot}s$), highest thermal conductivity (~5300 $W/m{\cdot}K$), and excellent optical transparency (~97.7%) make graphene a super material for electronics, optoelectronics, and etc.[1−7]

The carbon atoms in graphene are all chemically accessible. Hence chemistry, in particular covalent chemistry, provides a powerful pathway to tailor the physical properties of pristine graphene, making graphene stronger, more attractive, and going beyond.[8−16]

Graphene is built with an infinite number of benzene rings two-dimensionally. Similar to benzene, all the carbon atoms in graphene are $sp^2$ hybridized and contribute a $2p_z$ electron for $\pi$ bonding. Thus, various −C═C− double-bond reactions, including free radical addition[8,9,17−20] and cycloaddition[21−25] observed for benzene could be expected for graphene. However, there is still a remarkable difference between graphene and benzene because of the scale of $\pi$ electron conjugations. Graphene is a zero-gap semimetal, while benzene molecule has a large HOMO−LUMO gap. The $\pi$ electrons are highly delocalized in the plane of graphene, making graphene, especially mechanical exfoliated graphene, extremely inert for most of chemical reactions. Although CVD grown graphene and chemically derived graphene showed higher reactivity because of the presence of defects, a similar inertness with mechanical exfoliated graphene was predicted if the defects were removed.[26] Therefore, high-temperature and high-energy reagents were usually required to overcome the energy barrier for the covalent modification of graphene. In fact, only a few chemical reactions have been developed so far for graphene chemistry with limited reaction efficiency.

In this Perspective, we will focus on the practice of covalent chemistry for tailoring the graphene's properties toward electronic devices. Typical examples of covalent chemistry will be given for the purpose of modulating the energy band structure of zero-gap graphene. Going beyond, the possibility and space of creating new 2D materials from mother graphene will also be discussed. As a chemically tailorable one-atom-thick scaffold, 2D graphene superlattices can also be fabricated via periodic chemical modification, which makes up the last part of the perspective. Through the different angles of view in this Perspective, we hope to bridge the gap between chemists, materials scientists, and device players.

## BAND STRUCTURE ENGINEERING

As predicted by Wallace in 1947,[27] graphene is endowed with a unique band structure by the special 2D atomic arrangement with two $sp^2$ hybridized carbon atoms in one unit cell (Figure 1a,b). The $sp^2$ carbon atoms provide two orbitals, $\pi$ and $\pi^*$, to form the valence and conduction bands, respectively. These two bands are only allowed to touch at six points, called as Dirac points, because the orthogonal $\pi$ and $\pi^*$ orbitals do not overlap with each other, making graphene a zero bandgap

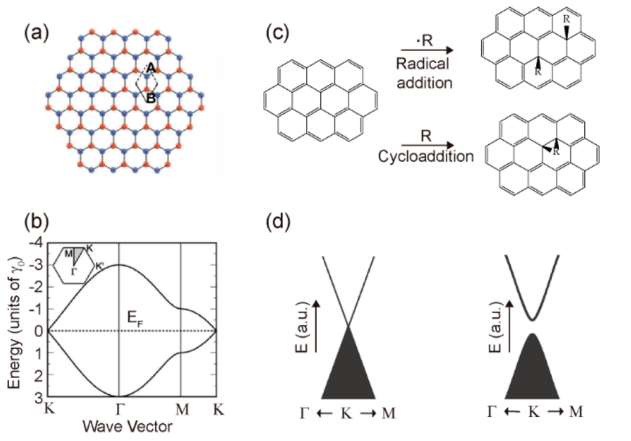


**Figure 1.** (a) Hexagonal honeycomb lattice of graphene with two carbon atoms (A and B) per unit cell. (b) Energy−momentum dispersion in graphene. (c) Schematic illustration of covalent chemistry of graphene. (d) Band structure change of single-layer graphene near the K point of the Brillouin zone before (left) and after (right) chemical modification. Panels (a) and (b) reproduced with permission from ref 34. Copyright, American Chemical Society 2010.

**Received:** May 14, 2014
**Published:** August 15, 2014

   dx.doi.org/10.1021/ja5048297 | J. Am. Chem. Soc. 2014, 136, 12194−12200

semimetal. The Dirac-cone band structures have linear energy−momentum dispersion near the Fermi level, which is most relevant with electron transport. Such a linear dispersion indicates that electrons in graphene exhibit zero rest mass, which is equivalent to the massless Fermions in the relativistic Dirac equation. In fact, graphene provides an ideal 2D system to investigate the intriguing physical phenomena involved in massless Dirac Fermions, e.g., the half-inter-quantum Hall effect.[28,29] Moreover, the massless electrons in graphene with a Fermi velocity of $\nu_F \approx 10^6$ m/s (1/300 the speed of light) have attracted much attention in electronic applications, such as radio frequency transistors[30,31] and ultrafast photodetectors.[32,33]

However, the zero bandgap nature of graphene results in a high leakage of currents and power dissipation, limiting its applications in standard logic circuits as a candidate for post-silicon electronics. In this regard, introduction of a bandgap in graphene through band structure engineering is highly desired. The zero bandgap structure of graphene arises from the symmetry of two carbon atoms in a unit cell. To open a bandgap, it is hence necessary to make the potential on the two atoms different.[30] Although a substantial bandgap (≥0.5 eV) and high on/off current ratio ($10^2$−$10^5$)[35−38] were obtained in the graphene nanoribbons (GNRs) with a width of 2−3 nm, the application of GNRs was limited because of the difficulties of experimental control on ribbon width and edge structure and of scalable production.

Chemical modification (Figure 1c,d) is an effective path to make the two carbon atoms in the unit cell of graphene distinguished from each other, thus opening the bandgap. Via covalent chemistry, the $sp^2$ hybridized carbon atoms are converted into $sp^3$ hybridized ones by forming a single bond with external groups. As mentioned above, many benzene-related reactions that break the −C═C− double bonds, e.g., free radical addition, would be lent for graphene modification. Haddon et al. developed a free radical addition path for the covalent modification of graphene using diazonium salts.[11] The aryl radicals dissociated from diazonium salts under heating broke the −C═C− double bonds and introduced aryl groups onto the graphene plane. Thus, tailored graphene supported on $SiO_2$/Si substrate behaved as a granular metal with a mobility gap of 0.1 eV at low temperature and a variable range hopping transport.[10] For the suspended graphene sample, which was expected to be modified in both sides by aryl groups, it was found to behave as a semiconductor with 80 meV gap at room temperature.[10]

Photoinduced free radical reactions were important routes for graphene's covalent chemistry.[39] The high-energy free radicals generated under light irradiation would facilitate the addition reaction of chemically inert graphene. From the device fabrication point of view, light is particularly attractive as a clean, easily operated, and patternable tool. Brus et al. pioneered the photoinduced graphene chemistry.[19] Starting from benzoyl peroxide, they introduced aryl groups onto the graphene scaffold via photo-assisted aryl radical addition. Our group also has made great efforts on the graphene photochemistry. Following a general concept of the photochemical bandgap engineering of graphene, we developed a number of effective reaction paths, including photochlorination,[9] photocatalytic oxidation,[15] and photomethylation[40] (Figure 2a).

The photochlorination reaction was inspired by the addition reaction between benzene and $Cl_2$ in the presence of light.[9,41] When graphene was exposed to $Cl_2$ gas under UV light, the

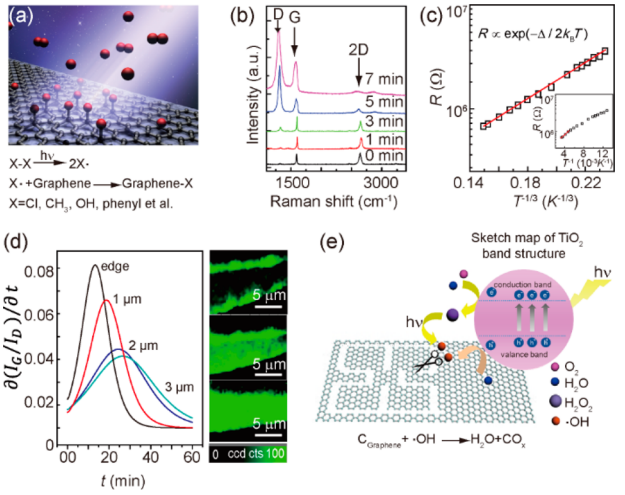


**Figure 2.** (a) Schematic illustration of graphene photochemistry based on photogenerated high-energy free radicals. (b) Raman spectral evolution of graphene upon photochlorination, where the rapid increase of D band intensity indicates the fast reaction kinetics. (c) Temperature dependence of electrical resistance of photochlorinated graphene. (d) Time evolution of photomethylation demonstrating that the reaction started from graphene edges. (e) Schematic of $TiO_2$-based photocatalytic oxidation of graphene, where the photogenerated hydroxyl radicals are employed as chemical scissors for graphene tailoring. Panels (b), (c) and (e) reproduced with permission from refs 9 and 18, respectively. Copyright, American Chemical Society 2011. Panel (d) reproduced with permission from ref 40. Copyright, Wiley 2013.

photogenerated Cl radicals were first adsorbed onto the graphene surface followed by a significant increase of electrical conductivity. After reaching a threshold concentration, addition reaction of Cl radicals occurred, forming a chlorinated graphene with ∼8 atom % Cl coverage. The photochlorination reaction was highly efficient as shown in Figure 2b, in which only a few minutes were required to reach the saturated coverage. The photochlorinated graphene derivative had a transport gap of ca. 45 meV (Figure 2c). Similar strategy also worked on the photomethylation of graphene by using di-*tert*-butyl peroxide as the methyl radical source.[40] In this case, the methyl groups could be removed from methylated graphene by heating up to 380 °C. Remarkably, the methyl addition reaction usually started from graphene edge, which could offer a unique pathway to synthesize graphene nanoribbons simply by narrowing the electrically conductive pristine graphene areas (Figure 2d). Another successful example of graphene photochemistry was the $TiO_2$-based photocatalytic oxidation reaction of graphene (Figure 2e).[18] With the aid of $TiO_2$ photocatalyst, highly reactive •OH radicals could be created under UV illumination with a suitable humidity. The hydroxyl radicals could readily convert graphene into graphene oxide, an electrically insulating material. By increasing the UV light intensity and irradiation time, the photogenerated hydroxyl radicals could work as sharp chemical scissors to completely cut graphene into nanoribbons and nanomesh structures, allowing for the versatile design and fabrication of graphene-based devices and circuits.

Cycloaddition reactions, for example, Diels−Alder (DA) reaction was an alternative way to break the −C═C− double bonds.[42,43] According to the frontier molecular orbital theory, the conduction and valence bands (HOMO and LUMO) of graphene cross at the Dirac point and provide a counterpart of


dx.doi.org/10.1021/ja5048297 | J. Am. Chem. Soc. 2014, 136, 12194−12200

donor−acceptor orbitals. Thus, the orbitals of graphene at the Dirac point are 2-fold degeneracy and half-filled, making graphene either a donor or an acceptor during the reaction by matching its antisymmetric (A) or symmetric (S) orbitals to those of its DA partner. Haddon and co-workers accomplished the DA reaction between graphene and tetracyanoethene, where graphene served as a diene.[42] In contrast, graphene was used as a dienphile in its DA reaction with 9-methylanthracene, which clearly showed the simultaneous transformation of a pair of neighboring $sp^2$ carbon atoms to 1,2-$sp^3$ hybridized structures.[42]

As a molecule with all atoms exposed, the reactivity of graphene is highly dependent on the surrounding environment. In fact, the HOMO and LUMO energy levels of graphene could be easily tuned using chemical doping or the external electric field effect, which led to the change of reactivity.[44] Strano et al. proved that the electron transfer between graphene and diazonium salt was greatly affected by the doping level of graphene. The n-type doped graphene exhibited a higher reactivity due to the higher Fermi level. They found that the reactivity of CVD grown graphene supported by $SiO_2$ substrate was higher than those on modified $SiO_2$ substrate and boron nitride (BN) because of the mild doping of the charge impurities on $SiO_2$ substrate.[44] Moreover, the $sp^2$ hybridized carbon networks with higher curvature, such as fullerene and carbon nanotubes, exhibited higher reactivity because of diminished electronic delocalization.[45] Ruoff et al. investigated the reactivity of curved graphene by introducing localized high curvature and proved that the curved area, usually the wrinkle of graphene, showed higher reactivity.[46] The compression or stretching of graphene would change the length of −C═C− double bonds, thus increasing the reactivity.[47] The stretching stress was successfully introduced into graphene supported on PDMS substrate and the reaction rate was dramatically increased (up to 10-fold).[26] Yet, the effect of compression stress, which has been predicted to be more efficient in increasing the reactivity than stretching stress, was not reported.

In brief, the covalent modification of graphene can provide a chemical path to make the two carbon atoms in a unit cell of graphene different from each other and thus open the bandgap. Although the delocalization of $\pi$ electrons makes graphene chemically inert, various reactions can still be successfully realized. In most cases, these reactions result in disordered modification, leading to the sharp decrease of carrier mobility. A balance between opening a bandgap and obtaining a desirable conductivity is required, which closely depends on the surface coverage of modified groups and the reaction nature.

## ■ GRAPHENE-DERIVED 2D MATERIALS

The interest in 2D materials, such as layered transition-metal oxides, metal chalcogenides, and metal halides, has been raised since the isolation of graphene. Because of the unique structures and properties, 2D materials have great potentials for optoelectronics, spintronics, catalysts, solar cells, and etc.

Graphene can serve as an excellent scaffold to build new 2D materials with designed structures and properties because all the $sp^2$ hybridized carbon atoms in graphene are chemically accessible, offering a versatile choice for chemical designs. Considering the typical hydrogenation reaction of olefins, it is reasonable to predict the possibility of graphane, a fully hydrogenated derivative of graphene. In fact, theoretical calculations have revealed that graphane was thermodynamically stable with a C:H ratio of 1:1.[49] Similar to cyclohexane, graphane had two stable conformations (Figure 3a,b):[48] a chair

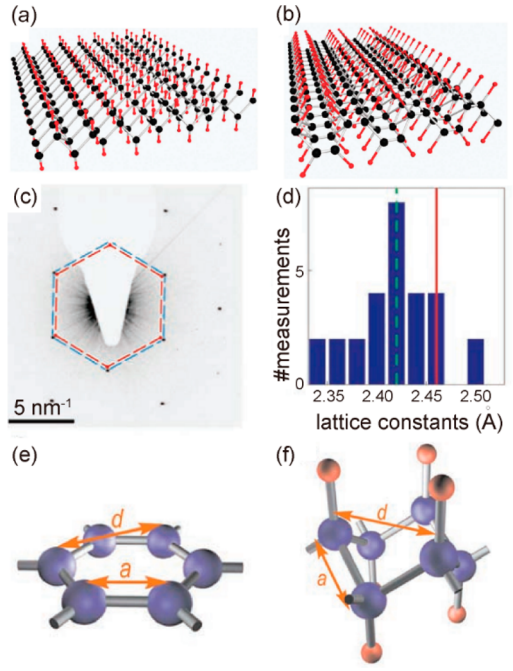


**Figure 3.** Chair (a) and boat (b) conformers of graphane. (c) Changes in the electron diffraction of graphane. The blue and red hexagons mark positions of the diffraction spots in graphane and graphene under the same conditions, respectively. (d) Distribution of the lattice constants found in hydrogenated graphene. The green dashed line marks the average value, whereas the red solid line shows lattice constants observed for graphene (both before hydrogenation and after annealing). (e) Schematic structure of graphene. (f) Schematic structure of theoretically predicted graphane. Panels (a) and (b) reproduced with permission from ref 48. Copyright, Royal Society of Chemistry 2012. Panels (c−f) reproduced with permission from ref 11. Copyright, American Association for the Advancement of Science 2009.

conformer and a boat conformer with the former being slightly more stable than the latter. Each of these two conformers had a direct bandgap at the K point with 3.5 eV for the chair conformer and 3.7 eV for the boat conformer.[49] Geim et al. made the first synthesis of graphane by a hydrogenation reaction of graphene.[11] By exposing hydrogen plasma onto the free-standing graphene, they succeeded in double-sided hydrogenation of graphene. The high-energy hydrogen atoms broke the $\pi$-electron conjugation system of graphene and converted the carbon configuration from $sp^2$ to $sp^3$. The transmission electron microscopy (TEM) results (Figure 3c,d) revealed that the as-prepared graphane had a hexagonal symmetry with a lattice constant $d = 2.46 \pm 0.02$ Å, which was 1% smaller than that of graphene. The decrease of lattice constant after hydrogenation originated from the change of carbon configuration from $sp^2$ (Figure 3e) to $sp^3$ (Figure 3f). The $d$ value was not uniform in the whole area, indicating that the experimentally produced graphane might be polycrystalline rather than single crystalline. In addition, the bonded H atoms could be lost at moderate temperatures with the restoring of $\pi$ electron conjugation. The Raman spectra showed that the strong D band disappeared after dehydrogenation, indicating the structural recovery of graphene. Such a reversible


dx.doi.org/10.1021/ja5048297 | J. Am. Chem. Soc. 2014, 136, 12194−12200

hydrogenation−dehydrogenation property may offer additional controllability of the conductivity in graphene devices. Moreover, graphane had a huge hydrogen density, which may make it as the hydrogen storage material for hydrogen fuel technology.

Another representative example of 2D materials derived from mother graphene is fluorographene, a fully fluorinated graphene via addition reaction of −C═C− double bonds. The hint may come from the well-known fully fluorinated analogues, such as Teflon (polytetrafluoroethylene) and graphite fluoride.[49−51] Theoretical simulation showed that fluorographene, a 2D Teflon, also had two stable conformations, in which the chair conformer (Figure 4a) was more stable than the boat

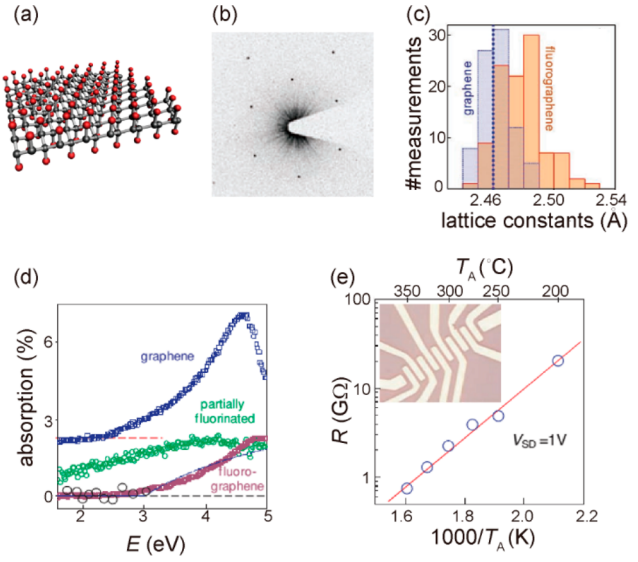


**Figure 4.** (a) Chair conformer of fluorographene. (b) Diffraction pattern from fluorographene. (c) Lattice constant measured from diffraction patterns. The dotted line indicates lattice constants for graphite. (d) Optical transparency change of graphene due to fluorination. The solid curve is the absorption behavior expected for a 2D semiconductor with $E_g$ = 3 eV. (e) Changes in fluorographene's $\rho$ induced by annealing. No current was detected at a temperature below 200 °C. At higher temperature, $\rho$ fell below 1 T Ω and became measurable in the experiments. Panels (b−e) reproduced with permission from ref 12. Copyright, Wiley 2010.

conformer. Several methods had been developed to covalently bond fluorine atoms onto graphene scaffold.[9,10,17] A highly reactive $XeF_2$ gas was proved effective to convert suspended graphene into fluorographene with a fluorine atomic percentage of 50%.[9,10] TEM data clearly showed that the unit cell of fluorographene was approximately 1% larger than graphene because fluorination resulted in $sp^3$-type bonding which had a larger interatomic distance than $sp^2$ one (Figure 4b,c).[12] Fluorographene was found to be transparent at most visible frequencies and absorbed light only in the blue range, indicating that fluorographene was a wide-gap semiconductor with $E_g \geq$ 3.0 eV (Figure 4d). Fluorographene exhibited an insulating behavior, and no current was detected at temperature below 200 °C (Figure 4e). At higher temperature, the electrical resistance $\rho$ fell below 1 T Ω and became measurable in the experiments, attributable to desorption of fluoride atoms and recovery of graphene. The structure of graphene could also be restored just as that with graphane, after electron beam irradiation[52] or chemical reaction.[53]

Despite of the successful synthesis of graphane and fluorographene, new 2D graphene derivatives with fascinating properties had significant challenges in synthesis because of the steric hindrance to the addition elements. Atoms with large size such as Cl and Br after addition could overlap with each other and reduce the stability.[54] Chlorographene was predicted less stable than graphane and fluorographene.[55] So far, the experimental coverage of chlorinated graphene was only ca. 8%, far from fully chlorination value.[9,56] The synthesis of fully chlorinated graphene has not been reported yet. Metallic bromographene was predicted to be highly unstable.[54,57,58] Brominated graphene with only a coverage of 4.8% was prepared by UV irradiation in bromine medium.[59,60] To expand the 2D graphene derivative family, the pseudo halogens, such as $(CN)_2$ and $(OCN)_2$, might also be applicable since these functional groups share similar properties with halogen atoms but have much smaller sizes.[61]

Interestingly, the one atom thick structure and perfect impermeability make it possible to modify graphene with different decorations on each side (Figure 5a). Such kind of

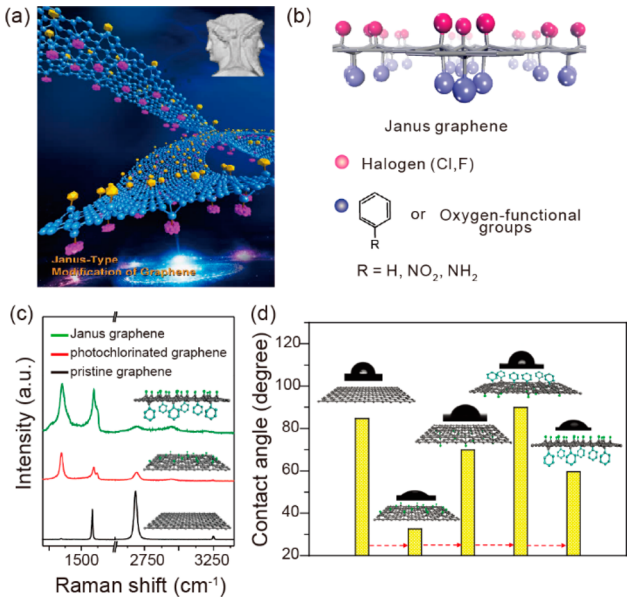


**Figure 5.** (a,b) Schematic structures of a Janus graphene. The red balls in (b) represent the Cl or F atoms covalent attached on one side of the as-prepared Janus graphene, and the blue balls represent the oxygen-functional groups or the different phenyl groups. (c) Raman spectral changes of graphene following one- and two-sided asymmetric modifications. (d) Static water contact angle changes of single-atom-thick 2D graphene derivatives. Reproduced with permission from ref 64. Copyright, Nature Publishing Group 2013.

asymmetrically modified graphene may provide additional attractions. The half-hydrogenated and half-fluorinated graphene was predicted as a semiconductor with a direct bandgap that was smaller than that of graphane but larger than fluorographene.[62] We had theoretically studied a series of Janus graphene (Figure 5b), the asymmetrically modified graphene by two different species, e.g., H, F, Cl, Br, and phenyl.[63,64] It was found that the asymmetric modification broke the symmetric restrictions of graphene, resulting in a robust nonzero bandgap, which was nearly linearly correlated with the binding energy of two functionalities. Experimentally, we achieved the first asymmetric functionalization of graphene


dx.doi.org/10.1021/ja5048297 | J. Am. Chem. Soc. 2014, 136, 12194−12200

through two-step covalent modification (Figure 5c).[64] With only one atom thickness, the surface properties such as wettability could be remarkably altered by chemical modification of the opposite side (Figure 5d). Because of the spatial restrictions, asymmetric modification of graphene with phenyl and chorine groups cannot reach higher surface coverage. It is highly expected for a high-coverage Janus graphene decorated by hydrogen and fluorine atoms.

## 2D GRAPHENE SUPERLATTICE

A superlattice is a periodic structure made up of alternating layers of two (or more) materials, whose thickness lies within 1−10 nm (about 10−100 atom layers). The combination of such thin materials endows new fascinating properties to the superlattice. Different from the classical 3D superlattice, a 2D superlattice is an in-plane periodic structure of two different materials with a periodicity of tens to hundreds of nanometers, in which the electrons behave similar to electrons in an atomic crystal with square lattice. Such novel structure provides an ideal platform to study the rich physics expected in 2D electronic systems.[65]

Unlike conventional 2D superlattices, the graphene superlattice sparked interests because the charge carriers confined on the surface could be easily tuned through physical and chemical modifications. A typical graphene superlattice was the *mosaic* structure composed of graphene and hexagonal boron nitride (hBN) (Figure 6a). We theoretically investigated the electronic structures of hBN-embedded graphene superlattices.[66,67] Such structures exhibited ubiquitous opened gaps governed by the width ($W$) of the wall between BN quantum dots (QDs). One of the most important features of such superlattice structures might be the extremely high carrier mobilities together with the gap opening, which was essential for fabricating graphene-based high-performance electronic devices.[67] The theoretical calculations showed that the intrinsic carrier mobility at room temperature was tunable from $1.7 \times 10^3$ to $1.1 \times 10^5$ $cm^2\ V^{-1}\ s^{-1}$ with a bandgap of 0.38−1.39 eV.[67] The *mosaic graphene* was experimentally obtained by alternatively growing pristine and n-type doped graphene using methane and acetonitrile as the carbon source, respectively (Figure 6b).[68] Although the periodicity of thus-prepared mosaic graphene was much larger than that of 2D superlattices, this direct growth approach was promising to further improve the electronic performances by reducing the size of periodic structures. If the embedded hBN islands in Figure 6a were removed, a mesh-like structure, called as graphene nanomesh, was obtained, which had a substantial bandgap sensitive to the width between the neighboring holes.[69−72]

Site-selective periodic chemical modification of graphene scaffold provided a straightforward way to fabricate 2D graphene superlattices (Figures 6c). A number of examples could be found along this direction.[9,18,20,50,73,74] A photochemical reaction path would simplify such patterned chemical modifications by the use of photomask. We developed a photochlorination reaction process for this purpose.[9] The 2D superlattice structure could be achieved under masked photochlorination, where the UV light-exposed areas were selectively chlorinated via addition reaction of photogenerated highly reactive chlorine radicals, while the unexposed areas remained intact. As shown in Figure 6d, the Raman D band mapping of graphene clearly showed the formation of 2D superlattice. Similarly, the $TiO_2$-based photocatalytic oxidation process could also be employed for fabricating 2D graphene

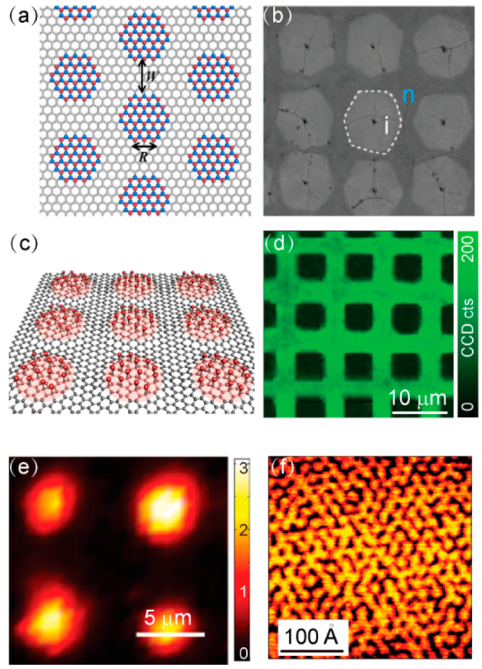


**Figure 6.** (a) Schematic illustration of hBN-embedded graphene superlattice, $R$ represents the radius of hexagonal BN quantum dots and $W$ represents the width of the wall. (b) SEM image of experimentally grown pristine (i) and nitrogen-doped (n) graphene superlattice. (c) Cartoon drawing of $TiO_2$-based photocatalysis-induced graphene oxide patterns on graphene matrix. (d) Raman D band mapping on CVD-grown graphene after patterned photochlorination, the green area is chlorinated with higher D band intensity and the black area is pristine. (e) Raman D/G intensity ratio mapping of CVD graphene after photocatalytic oxidation using a circular $TiO_2$ photomask, the red cycle represent the modified area with larger D/G ratio and the black are remains pristine. (f) STM image of Moiré patterns on graphene/Ir(111) substrate after exposed to hydrogen atoms for 50 s. Panels (a), (d), and (e) are reproduced with permission from refs 66, 9, and 18, respectively. Copyright, American Chemical Society 2012, 2011, and 2011. Panels (b) and (f) are reproduced with permission from refs 68 and 74, respectively. Copyright, Nature Publishing Group 2013 and 2010.

superlattices.[18] In this case, the photogenerated •OH radicals attacked the exposed graphene area and converted it into graphene oxide. The 2D superlattice structure consisted of intrinsic graphene matrix and embedded regular oxide islands (Figure 6e). The technical challenge for the photomask-derived graphene patterning is the subdiffraction-limited transverse feature sizes. Although the periodicities of the 2D superlattices are several micron, which is limited by the technology, typical 2D graphene superlattices with sizes ranging from a few microns down to tens of nanometers are available with the breakthrough in patterning methods.

Graphene's chemical reactivity is strongly affected by the underlying substrate because of its atomically thin nature. This can be used for fabricating 2D graphene superlattices with nanometer scale feature size. For instance, as a single layer graphene grown on Ir(111) surface, a moiré pattern, attributed to the geometric and electronic effect of the substrate, could be observed. Such Moiré superlattice could induce a patterned adsorption of hydrogen atoms on graphene.[74] The presence of hydrogen atoms resulted in rehybridization of graphenic carbons from $sp^2$ to $sp^3$. These rehybridized carbon atoms created chemical bonds with either the hydrogen adsorbates or


dx.doi.org/10.1021/ja5048297 | J. Am. Chem. Soc. 2014, 136, 12194−12200

the underlying Ir atoms. Arising from such a chemical reconstruction, a number of protrusions (Figure 6f) appeared on the bright parts of moiré pattern after exposed graphene/Ir(111) to hydrogen. Together with the increase of hydrogen dose, a ring-like structure along the moiré pattern was observed and an elongated structure was formed at high hydrogen doses. The angle-resolved photoelectron spectroscopy measurements indicated the formation of a tunable bandgap within such 2D graphene superlattice.[73] A significant gap of at least 450 meV was observed when the dose of atomic hydrogen increased.

In addition to above chemical approaches, a physical modulation can also be utilized for building graphene superlattice, e.g., by introducing a periodic potential via substrate or external electrical field.[65,75] Hornekær et al. transferred graphene onto hBN, on which worked as the periodic potential.[74] Such Moiré pattern led to profound changes in the graphene's electronic spectrum. Deshmukh et al.[75] developed a lateral superlattice in a graphene device with a tunable barrier height through a combination of two gates. By introducing a periodic potential, new Dirac cones were created in graphene. It should be noted that such physical approaches only temporarily shifted the Fermi level but did not change the intrinsic structure of graphene.

The periodic modulation of graphene lattice by covalent chemical modification is no doubt an effective pathway to tune the bandgap of graphene. Unfortunately, the feature sizes of most periodic structures obtained so far are too large to tune the bandgap. To improve the electrical performance of 2D graphene superlattice, a nanometer scale feature size is highly desirable, which calls for the technological breakthrough. One of the promising approaches is the use of strain-enhanced reactivity of graphene. It is expected that the designed surface nanostructures, e.g., nanosphere arrays, would enable the nanometer scale modification of graphene by inducing highly localized chemical reactions.

## ■ CONCLUSION AND PERSPECTIVE

Covalent chemistry offers an effective pathway to the band structure modulation of graphene, opening a substantial band gap on the zero-gap electronic band of pristine graphene. The general challenge remained along this direction is the enhancement of reaction efficiency. One also needs to face the severe carrier mobility drop accompanied by the covalent modification of graphene, which sacrificed the major merits of graphene-based electronic devices. Using the graphene scaffold, new 2D materials and 2D graphenic superlattices with fascinating properties can be create based on a well-controlled covalent modification, which provides an attractive route to go beyond graphene. It is no doubt that there is still a broad space for graphene players on the covalent graphene chemistry toward new materials and electronic applications.

## ■ AUTHOR INFORMATION

### Corresponding Authors

zfliu@pku.edu.cn
hlpeng@pku.edu.cn

### Notes

The authors declare no competing financial interest.

## ■ ACKNOWLEDGMENTS

This work was financially supported by the Ministry of Science and Technology of China (Grants 2013CB932603, 2012CB933404, 2011CB933003), the National Natural Science Foundation of China (Grants 51290272, 51121091), and the Ministry of Education (20120001130010).

## ■ REFERENCES

(1) Bolotin, K. I.; Sikes, K. J.; Jiang, Z.; Klima, M.; Fudenberg, G.; Hone, J.; Kim, P.; Stormer, H. L. *Solid State Commun.* **2008**, *146*, 351.
(2) Du, X.; Skachko, I.; Barker, A.; Andrei, E. Y. *Nat. Nanotechnol.* **2008**, *3*, 491.
(3) Balandin, A. A.; Ghosh, S.; Bao, W. Z.; Calizo, I.; Teweldebrhan, D.; Miao, F.; Lau, C. N. *Nano Lett.* **2008**, *8*, 902.
(4) Nair, R. R.; Blake, P.; Grigorenko, A. N.; Novoselov, K. S.; Booth, T. J.; Stauber, T.; Peres, N. M. R.; Geim, A. K. *Science* **2008**, *320*, 1308.
(5) Huang, X.; Yin, Z.; Wu, S.; Qi, X.; He, Q.; Zhang, Q.; Yan, Q.; Boey, F.; Zhang, H. *Small* **2011**, *7*, 1876.
(6) He, Q.; Wu, S.; Yin, Z.; Zhang, H. *Chem. Sci.* **2012**, *3*, 1764.
(7) Huang, X.; Qi, X.; Boey, F.; Zhang, H. *Chem. Soc. Rev.* **2012**, *41*, 666.
(8) Bekyarova, E.; Itkis, M. E.; Ramesh, P.; Berger, C.; Sprinkle, M.; de Heer, W. A.; Haddon, R. C. *J. Am. Chem. Soc.* **2009**, *131*, 1336.
(9) Li, B.; Zhou, L.; Wu, D.; Peng, H. L.; Yan, K.; Zhou, Y.; Liu, Z. F. *ACS Nano* **2011**, *5*, 5957.
(10) Zhang, H.; Bekyarova, E.; Huang, J. W.; Zhao, Z.; Bao, W. Z.; Wang, F. L.; Haddon, R. C.; Lau, C. N. *Nano Lett.* **2011**, *11*, 4047.
(11) Elias, D. C.; Nair, R. R.; Mohiuddin, T. M. G.; Morozov, S. V.; Blake, P.; Halsall, M. P.; Ferrari, A. C.; Boukhvalov, D. W.; Katsnelson, M. I.; Geim, A. K.; Novoselov, K. S. *Science* **2009**, *323*, 610.
(12) Nair, R. R.; Ren, W. C.; Jalil, R.; Riaz, I.; Kravets, V. G.; Britnell, L.; Blake, P.; Schedin, F.; Mayorov, A. S.; Yuan, S. J.; Katsnelson, M. I.; Cheng, H. M.; Strupinski, W.; Bulusheva, L. G.; Okotrub, A. V.; Grigorieva, I. V.; Grigorenko, A. N.; Novoselov, K. S.; Geim, A. K. *Small* **2010**, *6*, 2877.
(13) Robinson, J. T.; Burgess, J. S.; Junkermeier, C. E.; Badescu, S. C.; Reinecke, T. L.; Perkins, F. K.; Zalalutdniov, M. K.; Baldwin, J. W.; Culbertson, J. C.; Sheehan, P. E.; Snow, E. S. *Nano Lett.* **2010**, *10*, 3001.
(14) Paredes, J. I.; Villar-Rodil, S.; Martinez-Alonso, A.; Tascon, J. M. D. *Langmuir* **2008**, *24*, 10560.
(15) Ramanathan, T.; Abdala, A. A.; Stankovich, S.; Dikin, D. A.; Herrera-Alonso, M.; Piner, R. D.; Adamson, D. H.; Schniepp, H. C.; Chen, X.; Ruoff, R. S.; Nguyen, S. T.; Aksay, I. A.; Prud'homme, R. K.; Brinson, L. C. *Nat. Nanotechnol.* **2008**, *3*, 327.
(16) Gao, W.; Alemany, L. B.; Ci, L. J.; Ajayan, P. M. *Nat. Chem.* **2009**, *1*, 403.
(17) Sarkar, S.; Bekyarova, E.; Haddon, R. C. *Angew. Chem., Int. Ed.* **2012**, *51*, 4901.
(18) Zhang, L. M.; Diao, S. O.; Nie, Y. F.; Yan, K.; Liu, N.; Dai, B. Y.; Xie, Q.; Reina, A.; Kong, J.; Liu, Z. F. *J. Am. Chem. Soc.* **2011**, *133*, 2706.
(19) Liu, H. T.; Ryu, S. M.; Chen, Z. Y.; Steigerwald, M. L.; Nuckolls, C.; Brus, L. E. *J. Am. Chem. Soc.* **2009**, *131*, 17099.
(20) Lee, W. H.; Suk, J. W.; Chou, H.; Lee, J. H.; Hao, Y. F.; Wu, Y. P.; Piner, R.; Aldnwande, D.; Kim, K. S.; Ruoff, R. S. *Nano Lett.* **2012**, *12*, 2374.
(21) Georgakilas, V.; Bourlinos, A. B.; Zboril, R.; Steriotis, T. A.; Dallas, P.; Stubos, A. K.; Trapalis, C. *Chem. Commun.* **2010**, *46*, 1766.
(22) Liu, L. H.; Zorn, G.; Castner, D. G.; Solanki, R.; Lerner, M. M.; Yan, M. D. *J. Mater. Chem.* **2010**, *20*, 5041.
(23) Quintana, M.; Spyrou, K.; Grzelczak, M.; Browne, W. R.; Rudolf, P.; Prato, M. *ACS Nano* **2010**, *4*, 3527.
(24) Ismaili, H.; Geng, D.; Sun, A. X.; Kantzas, T. T.; Workentin, M. S. *Langmuir* **2011**, *27*, 13261.
(25) Zhong, X.; Jin, J.; Li, S. W.; Niu, Z. Y.; Hu, W. Q.; Li, R.; Ma, J. T. *Chem. Commun.* **2010**, *46*, 7340.
(26) Bissett, M. A.; Tsuji, M.; Ago, H. *J. Phys. Chem. C* **2013**, *117*, 3152.
(27) Wallace, P. R. *Phys. Rev.* **1947**, *71*, 476.

(28) Zhang, Y. B.; Tan, Y. W.; Stormer, H. L.; Kim, P. *Nature* **2005**, *438*, 201.
(29) Novoselov, K. S.; Jiang, Z.; Zhang, Y.; Morozov, S. V.; Stormer, H. L.; Zeitler, U.; Maan, J. C.; Boebinger, G. S.; Kim, P.; Geim, A. K. *Science* **2007**, *315*, 1379.
(30) Lin, Y. M.; Dimitrakopoulos, C.; Jenkins, K. A.; Farmer, D. B.; Chiu, H. Y.; Grill, A.; Avouris, P. *Science* **2010**, *327*, 662.
(31) Liao, L.; Lin, Y. C.; Bao, M. Q.; Cheng, R.; Bai, J. W.; Liu, Y. A.; Qu, Y. Q.; Wang, K. L.; Huang, Y.; Duan, X. F. *Nature* **2010**, *467*, 305.
(32) Mueller, T.; Xia, F. N. A.; Avouris, P. *Nat. Photonics* **2010**, *4*, 297.
(33) Xia, F. N.; Mueller, T.; Lin, Y. M.; Avouris, P. Lasers and Electro-Optics (CLEO) and Quantum Electronics and Laser Science (QELS) Conference, San Jose, CA, May 16−21, 2010; IEEE: New York, 2010.
(34) Avouris, P. *Nano Lett.* **2010**, *10*, 4285.
(35) Wang, X. R.; Ouyang, Y. J.; Li, X. L.; Wang, H. L.; Guo, J.; Dai, H. J. *Phys. Rev. Lett.* **2008**, *100*, 20683.
(36) Li, X. L.; Wang, X. R.; Zhang, L.; Lee, S. W.; Dai, H. J. *Science* **2008**, *319*, 1229.
(37) Kosynkin, D. V.; Higginbotham, A. L.; Sinitskii, A.; Lomeda, J. R.; Dimiev, A.; Price, B. K.; Tour, J. M. *Nature* **2009**, *458*, 872.
(38) Jiao, L. Y.; Zhang, L.; Wang, X. R.; Diankov, G.; Dai, H. J. *Nature* **2009**, *458*, 877.
(39) Zhang, L. M.; Zhou, L.; Yang, M. M.; Liu, Z. R.; Xie, Q.; Peng, H. L. *Small* **2013**, *9*, 1134.
(40) Liao, L.; Song, Z. H.; Zhou, Y.; Wang, H.; Xie, Q.; Peng, H. L.; Liu, Z. F. *Small* **2013**, *9*, 1348.
(41) Zhou, L.; Zhou, L.; Yang, M.; Wu, D.; Liao, L.; Yan, K.; Xie, Q.; Liu, Z.; Peng, H.; Liu, Z. *Small* **2013**, *9*, 2485.
(42) Sarkar, S.; Bekyarova, E.; Niyogi, S.; Haddon, R. C. *J. Am. Chem. Soc.* **2011**, *133*, 3324.
(43) Sarkar, S.; Bekyarova, E.; Haddon, R. C. *Acc. Chem. Res.* **2012**, *45*, 673.
(44) Wang, Q. H.; Jin, Z.; Kim, K. K.; Hilmer, A. J.; Paulus, G. L. C.; Shih, C. J.; Ham, M. H.; Sanchez-Yamagishi, J. D.; Watanabe, K.; Taniguchi, T.; Kong, J.; Jarillo-Herrero, P.; Strano, M. S. *Nat. Chem.* **2012**, *4*, 724.
(45) Boukhvalov, D. W.; Katsnelson, M. I. *J. Phys. Chem. C* **2009**, *113*, 14176.
(46) Wu, Q. Z.; Wu, Y. P.; Hao, Y. F.; Geng, J. X.; Charlton, M.; Chen, S. S.; Ren, Y. J.; Ji, H. X.; Li, H. F.; Boukhvalov, D. W.; Piner, R. D.; Bielawski, C. W.; Ruoff, R. S. *Chem. Commun.* **2013**, *49*, 677.
(47) Boukhvalov, D. W.; Son, Y. W. *ChemPhysChem* **2012**, *13*, 1463.
(48) Yan, L.; Zheng, Y. B.; Zhao, F.; Li, S. J.; Gao, X. F.; Xu, B. Q.; Weiss, P. S.; Zhao, Y. L. *Chem. Soc. Rev.* **2012**, *41*, 97.
(49) Sofo, J. O.; Chaudhari, A. S.; Barber, G. D. *Phys. Rev. B* **2007**, *75*, 153401.
(50) Ryu, S.; Han, M. Y.; Maultzsch, J.; Heinz, T. F.; Kim, P.; Steigerwald, M. L.; Brus, L. E. *Nano Lett.* **2008**, *8*, 4597.
(51) Charlier, J. C.; Gonze, X.; Michenaud, J. P. *Phys. Rev. B* **1993**, *47*, 16162.
(52) Withers, F.; Bointon, T. H.; Dubois, M.; Russo, S.; Craciun, M. F. *Nano Lett.* **2011**, *11*, 3912.
(53) Zbořil, R.; Karlický, F.; Bourlinos, A. B.; Steriotis, T. A.; Stubos, A. K.; Georgakilas, V.; Šafářová, K.; Jančík, D.; Trapalis, C.; Otyepka, M. *Small* **2010**, *6*, 2885.
(54) Karlický, F.; Zbořil, R.; Otyepka, M. *J. Chem. Phys.* **2012**, *137*, 034709.
(55) Rüdorff, W. Graphite Intercalation Compounds. In *Advances in Inorganic Chemistry and Radiochemistry*; Emcleus, J., Sharpe, A. G., Eds.; Academic Press: New York, 1959; Vol. *1*, pp 233−266.
(56) Wu, J.; Xie, L.; Li, Y.; Wang, H.; Ouyang, Y.; Guo, J.; Dai, H. *J. Am. Chem. Soc.* **2011**, *133*, 19668.
(57) Klintenberg, M.; Lebegue, S.; Katsnelson, M. I.; Eriksson, O. *Phys. Rev. B* **2010**, *81*, 085433.
(58) Medeiros, P. V. C.; Mascarenhas, A. J. S.; Mota, F. D.; de Castilho, C. M. C. *Nanotechnology* **2010**, *21*, 485701.
(59) Zheng, J.; Liu, H. T.; Wu, B.; Di, C. A.; Guo, Y. L.; Wu, T.; Yu, G.; Liu, Y. Q.; Zhu, D. B. *Sci. Rep.* **2012**, *2*, 662.
(60) Gopalakrishnan, K.; Subrahmanyam, K. S.; Kumar, P.; Govindaraj, A.; Rao, C. N. R. *Rsc. Adv.* **2012**, *2*, 1605.
(61) Karlicky, F.; Kumara Ramanatha Datta, K.; Otyepka, M.; Zboril, R. *ACS Nano* **2013**, *7*, 6434.
(62) Zhou, J.; Wu, M. M.; Zhou, X.; Sun, Q. *Appl. Phys. Lett.* **2009**, *95*, 103108.
(63) Yang, M. M.; Zhao, R. Q.; Wang, J. Y.; Zhang, L. M.; Xie, Q.; Liu, Z. F.; Liu, Z. R. *J. Appl. Phys.* **2013**, *113*, 084313.
(64) Zhang, L. M.; Yu, J. W.; Yang, M. M.; Xie, Q.; Peng, H. L.; Liu, Z. F. *Nat. Commun.* **2013**, *4*, 1443.
(65) Ponomarenko, L. A.; Gorbachev, R. V.; Yu, G. L.; Elias, D. C.; Jalil, R.; Patel, A. A.; Mishchenko, A.; Mayorov, A. S.; Woods, C. R.; Wallbank, J. R.; Mucha-Kruczynski, M.; Piot, B. A.; Potemski, M.; Grigorieva, I. V.; Novoselov, K. S.; Guinea, F.; Fal'ko, V. I.; Geim, A. K. *Nature* **2013**, *497*, 594.
(66) Zhao, R. Q.; Wang, J. Y.; Yang, M. M.; Liu, Z. F.; Liu, Z. R. *J. Phys. Chem. C* **2012**, *116*, 21098.
(67) Wang, J.; Zhao, R.; Liu, Z.; Liu, Z. *Small* **2013**, *9*, 1373.
(68) Yan, K.; Wu, D.; Peng, H.; Jin, L.; Fu, Q.; Bao, X.; Liu, Z. *Nat. Commun.* **2012**, *3*, 1280.
(69) Pedersen, T. G.; Flindt, C.; Pedersen, J.; Mortensen, N. A.; Jauho, A. P.; Pedersen, K. *Phys. Rev. Lett.* **2008**, *100*, 136804.
(70) Ouyang, F. P.; Peng, S. L.; Liu, Z. F.; Liu, Z. R. *ACS Nano* **2011**, *5*, 4023.
(71) Bai, J. W.; Zhong, X.; Jiang, S.; Huang, Y.; Duan, X. F. *Nat. Nanotechnol.* **2010**, *5*, 190.
(72) Liang, X. G.; Jung, Y. S.; Wu, S. W.; Ismach, A.; Olynick, D. L.; Cabrini, S.; Bokor, J. *Nano Lett.* **2010**, *10*, 2454.
(73) Sun, Z. Z.; Pint, C. L.; Marcano, D. C.; Zhang, C. G.; Yao, J.; Ruan, G. D.; Yan, Z.; Zhu, Y.; Hauge, R. H.; Tour, J. M. *Nat. Commun.* **2011**, *2*, 559.
(74) Balog, R.; Jorgensen, B.; Nilsson, L.; Andersen, M.; Rienks, E.; Bianchi, M.; Fanetti, M.; Laegsgaard, E.; Baraldi, A.; Lizzit, S.; Sljivancanin, Z.; Besenbacher, F.; Hammer, B.; Pedersen, T. G.; Hofmann, P.; Hornekær, L. *Nat. Mater.* **2010**, *9*, 315.
(75) Dubey, S.; Singh, V.; Bhat, A. K.; Parikh, P.; Grover, S.; Sensarma, R.; Tripathi, V.; Sengupta, K.; Deshmukh, M. M. *Nano Lett.* **2013**, *13*, 3990.